J|A|C|S
ARTICLES
Published on Web 02/06/2007

Glycosidase Inhibition: An Assessment of the Binding of 18 Putative Transition-State Mimics

Tracey M. Gloster,[†] Peter Meloncelli,[‡] Robert V. Stick,[‡] David Zechel,[§] Andrea Vasella,[||] and Gideon J. Davies*,[†]

Contribution from the York Structural Biology Laboratory, Department of Chemistry, University of York, York YO10 5YW, U.K., Chemistry, School of Biomedical, Biomolecular and Chemical Sciences M313, University of Western Australia, Crawley, Western Australia 6009, Australia, Department of Chemistry, Queen's University, Chernoff Hall, 90 Bader Lane, Kingston, Ontario K7L 3N6, Canada, and Laboratorium für Organische Chemie, HCI H 317, ETH-Zürich, CH-8093 Zürich, Switzerland

Received September 27, 2006; E-mail: davies@ysbl.york.ac.uk

Abstract: The inhibition of glycoside hydrolases, through transition-state mimicry, is important both as a probe of enzyme mechanism and in the continuing quest for new drugs, notably in the treatment of cancer, HIV, influenza, and diabetes. The high affinity with which these enzymes are known to bind the transition state provides a framework upon which to design potent inhibitors. Recent work [for example, Bülow, A. *et al. J. Am. Chem. Soc.* **2000**, *122*, 8567−8568; Zechel, D. L. *et al. J. Am. Chem. Soc.* **2003**, *125*, 14313−14323] has revealed quite confusing and counter-intuitive patterns of inhibition for a number of glycosidase inhibitors. Here we describe a synergistic approach for analysis of inhibitors with a single enzyme 'model system', the *Thermotoga maritima* family 1 β-glucosidase, *Tm*GH1. The pH dependence of enzyme activity and inhibition has been determined, structures of inhibitor complexes have been solved by X-ray crystallography, with data up to 1.65 Å resolution, and isothermal titration calorimetry was used to establish the thermodynamic signature. This has allowed the characterization of 18 compounds, all putative transition-state mimics, in order to build an 'inhibition profile' that provides an insight into what governs binding. In contrast to our preconceptions, there is little correlation of inhibitor chemistry with the calorimetric dissection of thermodynamics. The ensemble of inhibitors shows strong enthalpy−entropy compensation, and the random distribution of similar inhibitors across the plot of $\Delta H°_a$ vs $T\Delta S°_a$ likely reflects the enormous contribution of solvation and desolvation effects on ligand binding.

Glycosidase inhibition is important not only in the study of enzyme mechanism, but also in therapies targeted at, for example, cancer, viral infections including HIV and influenza, lysosomal storage diseases, and diabetes, with a number of drugs in current clinical use. Wolfenden has pointed out that glycoside hydrolases (hereafter glycosidases) are extremely exciting targets for inhibition through transition-state mimicry since their rate enhancements, estimated at over 10^{17} fold compared to the uncatalyzed reaction,[1] implies a binding constant for the transition state of around 10^{-22} M.[1] Notwithstanding the fact that the transition state involves non-ground-state bond lengths and partial charges, which may prove difficult to mimic appropriately, current glycosidase inhibitors are rather poor, with the best binding only in the low nanomolar range. Building on Pauling's proposals in the 1940s,[2,3] if compounds are designed to mimic this transition state, meaning more of the transition state binding potential is harnessed, then highly potent inhibitors could result. This has most recently been elegantly demonstrated by Schramm and co-workers, who have obtained pico- and femtomolar inhibitors (among the most potent of any noncovalently bound inhibitors reported) of enzymes (including 5′-methylthioadenosine/*S*-adenosylhomocysteine nucleosidases, *N*-ribosyltransferases, and purine nucleoside phosphorylases) using a combination of X-ray crystallography and computer modeling driven by transition state insight derived from kinetic isotope effects.[4−8]

Glycosidases provide a powerful tested system in which to study transition-state mimicry. Currently, they have been classified into over 100 families based upon amino-acid sequence similarities (see http://afmb.cnrs-mrs.fr/CAZY/).[9] Family GH1 glycosidases, such as the β-glucosidase from *Thermotoga maritima* (*Tm*GH1) described here, perform glycoside

[†] University of York.
[‡] University of Western Australia.
[§] Queen's University.
[||] Laboratorium für Organische Chemie.

(1) Wolfenden, R.; Lu, X.; Young, G. *J. Am. Chem. Soc.* **1998**, *120*, 6814−6815.
(2) Pauling, L. *Nature* **1946**, *24*, 1375−1377.
(3) Pauling, L. *Nature* **1948**, *161*, 707−709.
(4) Lee, J. E.; Singh, V.; Evans, G. B.; Tyler, P. C.; Furneaux, R. H.; Cornell, K. A.; Riscoe, M. K.; Schramm, V. L.; Howell, P. L. *J. Biol. Chem.* **2005**, *280*, 18274−18282.
(5) Schramm, V. L. *Biochim. Biophys. Acta* **2002**, *1587*, 107−117.
(6) Schramm, V. L. *Acc. Chem. Res.* **2003**, *36*, 588−596.
(7) Schramm, V. L. *Arch. Biochem. Biophys.* **2005**, *433*, 13−26.
(8) Singh, V.; Evans, G. B.; Lenz, D. H.; Mason, J. M.; Clinch, K.; Mee, S.; Painter, G. F.; Tyler, P. C.; Furneaux, R. H.; Lee, J. E.; Howell, P. L.; Schramm, V. L. *J. Biol. Chem.* **2005**, *280*, 18265−18273.

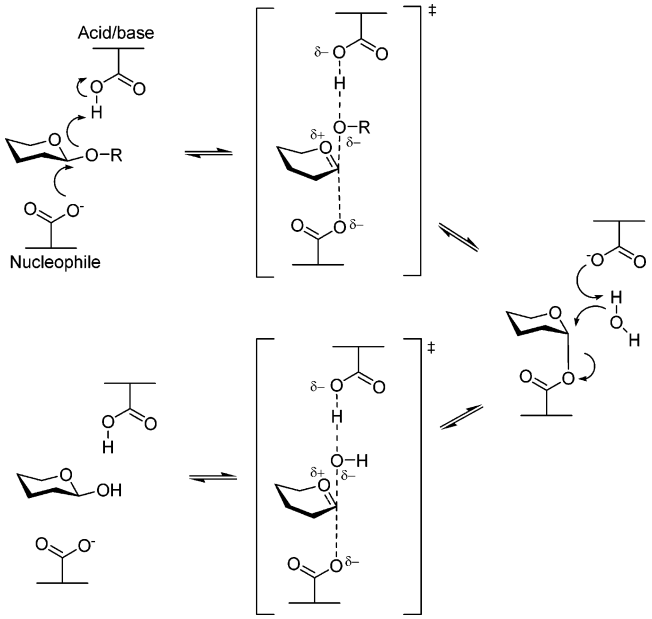

Figure 1. Canonical retaining mechanism for β-glycoside hydrolysis. Each step of the double displacement mechanism passes through a short-lived oxocarbenium ion-like transition state.

hydrolysis with net retention of anomeric configuration using a double displacement mechanism in which a covalent glycosyl-enzyme intermediate is formed and subsequently hydrolyzed *via* oxocarbenium ion-like transition states (Figure 1). Two key catalytic residues are involved: an acid/base, which first gives protonic assistance to leaving-group departure (and subsequently Brønsted base assistance to nucleophilic attack by water), and an enzymatic nucleophile responsible for the formation of the covalent glycosyl-enzyme intermediate. In the case of *Tm*GH1 both of these residues are glutamic acid residues. The transition state(s) for enzymatic glycoside hydrolysis displays sp^2 hybridization with a partial positive charge predominantly located across the C1−O5 bond. Sinnott[10] was perhaps the first to emphasize the stereochemical implication: that distortion of the glycoside to half-chair ($^4H_3$ and $^3H_4$ or their equivalent ^4E and ^3E envelope forms) or boat ($^{2,5}B$ or $B_{2,5}$) conformations is necessary at the transition state. Recent work has indeed now shown that different transition state conformations are adopted by different enzymes (Figure 2A, reviewed in ref 11), but there is widespread agreement that family GH1 enzymes, at least those acting on *gluco*-configured substrates, are likely to perform catalysis *via* a $^4H_3$ /^4E transition state conformation (Figure 2B).

A large number of glycosidase inhibitors are known. They have been isolated from natural sources or synthesized since the 1960s when the progenitor inhibitor nojirimycin was discovered (reviewed in refs 12−15). While tight binding of

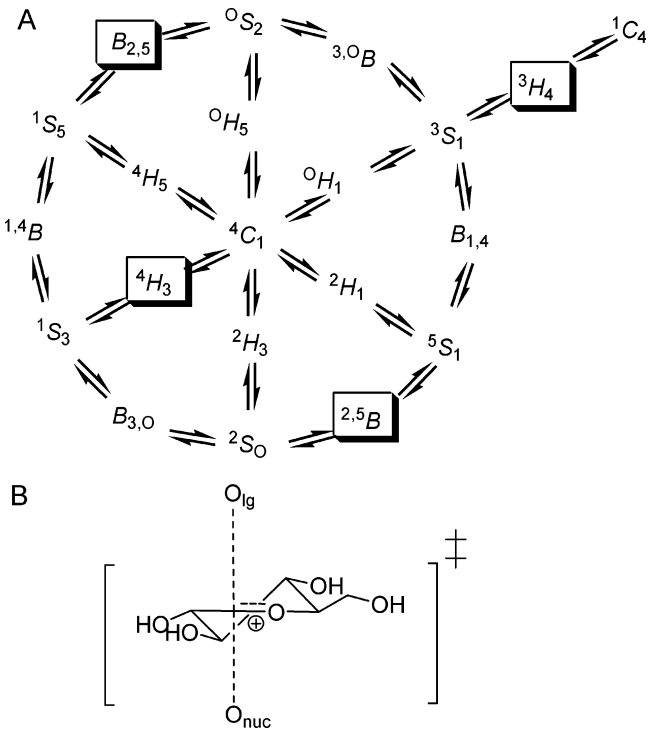

Figure 2. (A) Skew-boat interconversion itinerary for the hydrolysis of pyranosides. Stereochemical considerations demand distortion to $^4H_3$ or $^3H_4$ half-chair (or their equivalent ^4E and ^3E envelope forms) or $^{2,5}B$ or $B_{2,5}$ boat conformations (shown boxed) at the transition state. (B) It is widely assumed that family GH1 retaining β-glucosidases harness a $^4H_3$ transition state.

glycosidase inhibitors is almost always interpreted as reflecting mimicry of the transition state, it is really quite unclear which inhibitors are true mimics, which are merely adventitious binders, and, equally importantly, which features of these compounds actually give rise to potency. A number of different standpoints have been adopted, including an intuitive belief that obvious similarities between an inhibitor and the transition state must reflect mimicry *versus* a mathematically more rigorous position, based on the linear free energy work of Wolfenden and Bartlett (reviewed in ref 16), which suggests that changes in protein or inhibitor should be reflected in a correlation between K_i and k_{cat}/K_M. Wolfenden has also advocated a third criterion for transition-state mimicry inhibitor: binding should be associated with a large negative enthalpy of interaction, as is true of the real transition state.[17,18]

At a superficial level, glycosidase inhibitors tend to fall into two classes: those that may mimic the charge at the transition state and hence include a basic atom or group, and those which incorporate sp^2 hybridization in order to try and mimic the geometry of the transition state. Recently, however, it has become clear that the forces governing glycosidase inhibitor binding are complex, and occasionally counter-intuitive. Bols initially suggested that binding of isofagomine might actually be driven by entropy,[19] a thermodynamic signature clearly at odds with mimicry of the transition state, and while it has

(9) Coutinho, P. M.; Henrissat, B. Carbohydrate-active enzymes: an integrated database approach. In *Recent advances in carbohydrate bioengineering*; Gilbert, H. J., Davies, G. J., Henrissat, B., Svensson, B., Eds.; Royal Society of Chemistry: Cambridge, 1999; pp 3−12.
(10) Sinnott, M. L. *Chem. Rev.* **1990**, *90*, 1171−1202.
(11) Davies, G. J.; Ducros, V. M.-A.; Varrot, A.; Zechel, D. L. *Biochem. Soc. Trans.* **2003**, *31*, 523−527.
(12) Heightman, T. D.; Vasella, A. T. *Angew. Chem., Int. Ed.* **1999**, *38*, 750−770.
(13) Legler, G. *Adv. Carbohydr. Chem. Biochem.* **1990**, *48*, 319−384.
(14) Lillelund, V. H.; Jensen, H. H.; Liang, X.; Bols, M. *Chem. Rev.* **2002**, *102*, 515−553.
(15) Stütz, A. E. *Iminosugars as glycosidase inhibitors. Nojirimycin and beyond*; Wiley-VCH: Weinheim, 1999.
(16) Mader, M. M.; Bartlett, P. A. *Chem. Rev.* **1997**, *97*, 1281−1301.
(17) Snider, M.; Gaunitz, S.; Ridgway, C.; Short, S. A.; Wolfenden, R. *Biochemistry* **2000**, *39*, 9746−9753.
(18) Wolfenden, R.; Snider, M.; Ridgway, C.; Miller, B. *J. Am. Chem. Soc.* **1999**, *121*, 7419−7420.
(19) Bülow, A.; Plesner, I. W.; Bols, M. *J. Am. Chem. Soc.* **2000**, *122*, 8567−8568.

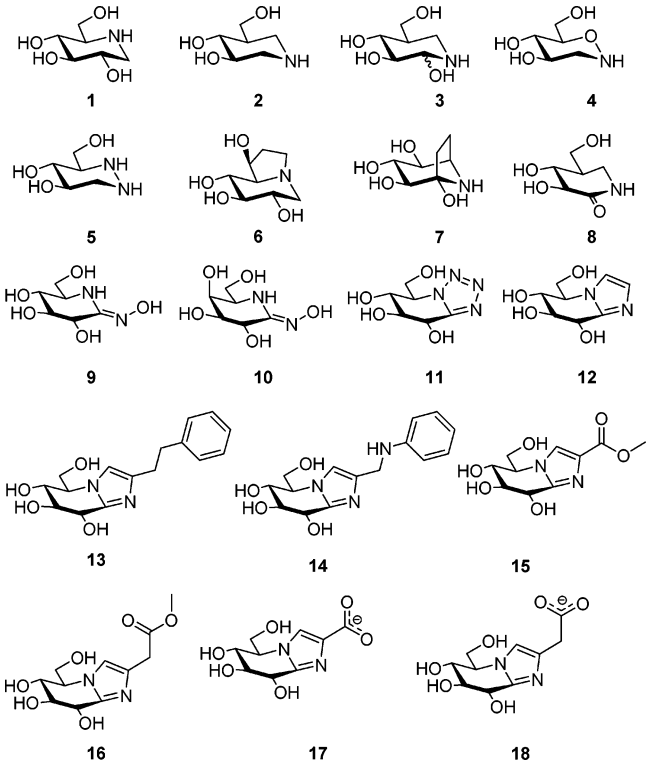

Figure 3. Structure of deoxynojirimycin **1**, isofagomine **2**, noeuromycin **3**, tetrahydrooxazine **4**, azafagomine **5**, castanospermine **6**, calystegine B_2 **7**, isofagomine lactam **8**, *gluco*-hydroximolactam **9**, *galacto*-hydroximolactam **10**, glucotetrazole **11**, glucoimidazole **12**, phenylethyl-substituted glucoimidazole **13**, phenylaminomethyl-substituted glucoimidazole **14**, methoxycarbonyl-substituted glucoimidazole **15**, methoxycarbonylmethyl-substituted glucoimidazole **16**, carboxylate-substituted glucoimidazole **17**, and carboxymethyl-substituted glucoimidazole **18**.

subsequently been demonstrated, by direct calorimetric measurement,[20] that isofagomine binding is enthalpically favorable, it none-the-less derives a large fraction of its potency from entropy. Similarly, the recent analysis of some glucoimidazole-derived glycosidase inhibitors again suggests quite complex binding signatures.[21] In light of these unusual results, here we have examined the inhibition of a single enzyme (*Tm*GH1) with 18 different glycosidase inhibitors (Figure 3) (partial data for eight of these have been reported in a preliminary form elsewhere[20−24]). The pH dependence of K_i is examined in light of the pH profile for catalysis itself for all 18 compounds. The three-dimensional structures of *Tm*GH1 in complex with **1**−**18** have also been determined by X-ray crystallography, at resolutions from 2.3 to 1.65 Å, and isothermal titration calorimetry (ITC) has been used to give an indication of the binding thermodynamics. Binding is characterized, as with many events, by strong enthalpy−entropy compensation. Our initial preconception was that inhibitors locked in the appropriate conformation would likely have shown both greater favorable enthalpy of interaction (by virtue of better transition-state mimicking interaction geometry) and perhaps also favorable entropy (by virtue of conformational restriction). What systematic analysis of these 18 compounds, whose K_i values range from 9 nM to 13 μM, actually shows is that there is no correlation between entropy of interaction and K_i, under the conditions used. Nor is there an obvious correlation between transition-state mimicry and enthalpy of interaction. Instead, inhibitors display a wide variety of thermodynamic signatures that do not correlate in a simple manner with the chemistry of the inhibitor itself, which likely reflects the difference in solvation and desolvation of the different compounds.

Materials and Methods

X-ray Crystallography. *Tm*GH1 was expressed, purified, and crystallized as described previously.[20] The *Tm*GH1 complexes were formed either by adding native crystals to a drop of mother liquor containing a minute amount of solid inhibitor and soaking for between 5 and 30 min, or by adding a minute amount of solid inhibitor to *Tm*GH1 prior to crystallization, and incubating for between 5 min and 2 h (see Supporting Information). Compounds **1** and **6** were purchased from Sigma, and the synthesis of the other compounds is described in the literature.[25−36] Crystals were cryoprotected in a solution containing the mother liquor with 25% ethylene glycol and frozen in liquid nitrogen.

Data for all complexes were collected at the ESRF, Grenoble. Data were processed and scaled with DENZO and SCALEPACK[37] (Supporting Information). All other calculations used the CCP4 suite of programs.[38] Isomorphism between the native *Tm*GH1 structure and the complexes meant refinement could commence following rigid body refinement in REFMAC[39] (using the protein atoms only from PDB entry 1OD0). Five percent of the observations were set aside for cross validation and were used to monitor refinement strategies.[40] Manual corrections of the model using COOT[41] were interspersed with cycles of least-squares refinement using REFMAC.[39]

Structure coordinates and structure factors have been deposited in the Protein DataBank with accession codes: 1OIM and 2J77 (**1**), 1OIF (**2**), 2J75 (**3**), 1W3J (**4**), 2J7H (**5**), 2CBU (**6**), 2CBV (**7**), 1UZ1 (**8**), 2J78 (**9**), 2J79 (**10**), 2J7B (**11**), 2CES (**12**), 2CET (**13**), 2J7C (**14**), 2J7D (**15**), 2J7E (**16**), 2J7F (**17**), and 2J7G (**18**).

Isothermal Titration Calorimetry. Isothermal titration calorimetry was performed using a VC calorimeter (Microcal, Northampton, MA) at 25 °C. *Tm*GH1 was dialyzed into 100 mM sodium citrate buffer, pH 5.8, and the inhibitors were diluted in the same buffer (Supporting Information). Samples were centrifuged and degassed prior to use. Titrations were performed by injecting 10 μL aliquots of ligand into

(20) Zechel, D. L.; Boraston, A. B.; Gloster, T.; Boraston, C. M.; Macdonald, J. M.; Tilbrook, D. M. G.; Stick, R. V.; Davies, G. J. *J. Am. Chem. Soc.* **2003**, *125*, 14313−14323.
(21) Gloster, T. M.; Roberts, S.; Perugino, G.; Rossi, M.; Moracci, M.; Panday, N.; Terinek, M.; Vasella, A.; Davies, G. J. *Biochemistry* **2006**, *45*, 11879−11884.
(22) Gloster, T. M.; Macdonald, J. M.; Tarling, C. A.; Stick, R. V.; Withers, S. G.; Davies, G. J. *J. Biol. Chem.* **2004**, *279*, 49236−49242.
(23) Gloster, T. M.; Madsen, R.; Davies, G. J. *ChemBiochem* **2006**, *7*, 738−742.
(24) Vincent, F.; Gloster, T. M.; Macdonald, J.; Morland, C.; Stick, R. V.; Dias, F. M. V.; Prates, J. A. M.; Fontes, C. M. G. A.; Gilbert, H. J.; Davies, G. J. *ChemBiochem* **2004**, *5*, 1596−1599.
(25) Best, W. M.; Macdonald, J. M.; Skelton, B. W.; Stick, R. V.; Tilbrook, D. M. G.; White, A. H. *Can. J. Chem.* **2002**, *80*, 857−865.
(26) Skaanderup, P. R.; Madsen, R. *J. Org. Chem.* **2003**, *68*, 2115−2122.
(27) Macdonald, J. M.; Stick, R. V. *Aust. J. Chem.* **2004**, *57*, 449−453.
(28) Ganem, B. *Acc. Chem. Res.* **1996**, *29*, 340−347.
(29) Hoos, R.; Naughton, A. B.; Thiel, W.; Vasella, A.; Weber, W.; Rupitz, K.; Withers, S. G. *Helv. Chim. Acta* **1993**, *76*, 2666−2686.
(30) Papandreou, G.; Tong, M. K.; Ganem, B. *J. Am. Chem. Soc.* **1993**, *115*, 11682−11690.
(31) Vonhoff, S.; Heightman, T. D.; Vasella, A. *Helv. Chim. Acta* **1998**, *81*, 1710−1725.
(32) Ermert, P.; Vasella, A. *Helv. Chim. Acta* **1991**, *74*, 2043−2053.
(33) Granier, T.; Panday, N.; Vasella, A. *Helv. Chim. Acta* **1997**, *80*, 979−987.
(34) Panday, N.; Canac, Y.; Vasella, A. *Helv. Chim. Acta* **2000**, *83*, 58−79.
(35) Shanmugasundaram, B.; Vasella, A. *Helv. Chim. Acta* **2005**, *88*, 2593−2602.
(36) Terinek, M.; Vasella, A. *Helv. Chim. Acta* **2004**, *87*, 3035−3049.
(37) Otwinowski, Z.; Minor, W. *Methods Enzymol.* **1997**, *276*, 307−326.
(38) Collaborative Computational Project Number 4. *Acta Crystallogr. D Biol. Crystallogr.* **1994**, *50*, 760−763.
(39) Murshudov, G. N.; Vagin, A. A.; Dodson, E. J. *Acta Crystallogr. D Biol. Crystallogr.* **1997**, *53*, 240−255.
(40) Brünger, A. T. *Nature* **1992**, *355*, 472−475.
(41) Emsley, P.; Cowtan, K. *Acta Crystallogr. D Biol. Crystallogr.* **2004**, *60*, 2126−2132.

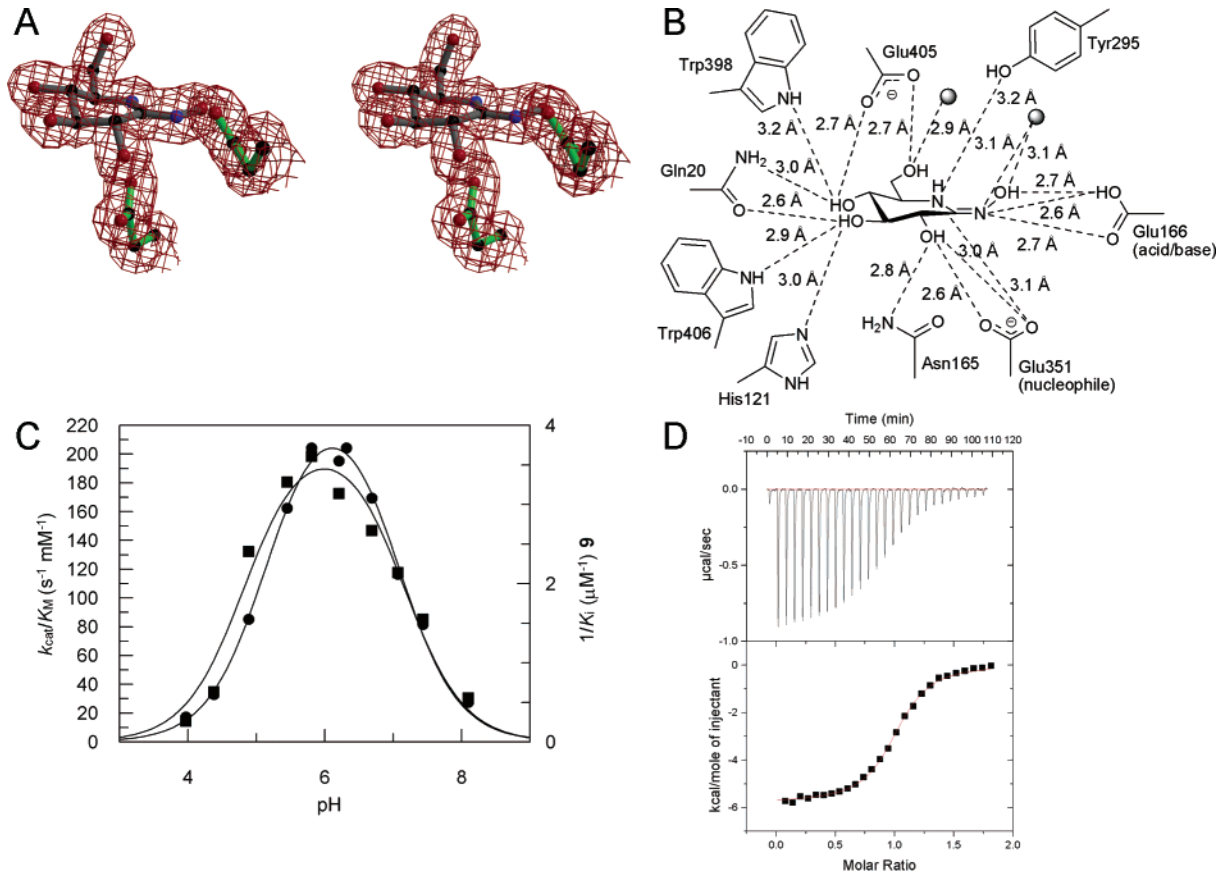

Figure 4. Structural, kinetic, and thermodynamic analysis of *Tm*GH1 with **9**. (A) Divergent stereo ball-and-stick representation of *Tm*GH1 [the nucleophile Glu351 (bottom) and acid/base Glu166 (right) are shown] in complex with **9**. Observed electron density for the maximum likelihood weighted $2F_{obs} - F_{calc}$ map is contoured at 1σ (~0.38 e Å^{-3}); the figure was drawn using BOBSCRIPT[83] and rendered using RASTER3D.[84] (B) Interactions made between *Tm*GH1 and **9**. (C) pH dependence of k_{cat}/K_M for *Tm*GH1 (filled circles) and $1/K_i$ for **9** (filled squares). Fits to bell-shaped ionization profiles are shown. (D) ITC data for **9** binding to *Tm*GH1. The top panel shows the raw titration data of the power supplied to the system to maintain a constant temperature against time; the area of the peak gives the heat of interaction for each injection. The bottom panel shows the bimolecular fit of the normalized heats of interaction plotted against the molar concentration.

*Tm*GH1. Data were corrected for the heat of dilution by subtracting the excess heat at high molar ratio of inhibitor to enzyme. The stoichiometry (n), enthalpy (ΔH), and equilibrium association constant (K_a) were determined from fitting to a bimolecular model using Microcal Origin software. The Gibbs free energy (ΔG) and entropy ($T\Delta S$) were calculated using the equations $\Delta G = -RT \ln K_a = \Delta H - T\Delta S$.

Kinetics. Kinetic studies with *Tm*GH1 were conducted by monitoring the change in UV/visible absorbance with a Cintra 10 spectrophotometer, equipped with a Thermocell Peltier power supply at 25 °C. k_{cat}/K_M dependence on pH for *Tm*GH1 was measured using substrate depletion methods at a substrate concentration lower than the K_M. Reactions were carried out at pH values ranging from pH 4 to 8 with 100 mM sodium citrate buffer or 100 mM sodium phosphate buffer. Typically assays contained 15 μM 2,4-dinitrophenyl β-D-glucopyranoside as substrate and 1 mg mL^{-1} bovine serum albumin (except at pH values below pH 5 where precipitation occurs), in a total volume of 1 mL. The reaction was initiated by addition of 10 μL of *Tm*GH1 to a final concentration of 3.4 nM, and 2,4-dinitrophenolate release was monitored continuously at 400 nm for a 600 s period. Data were fitted to a first-order rate equation using GRAFIT[42] to give V_{max}/K_M and adjusted for the enzyme concentration to obtain k_{cat}/K_M. Data at different pH values were fitted to a bell-shaped ionization curve. K_i values for all inhibitors with *Tm*GH1 were determined over the same pH range by monitoring the rates in the absence (v_0) and presence (v_i) of inhibitor under steady-state conditions (except for **1** and **4**, which are described in refs 22 and 20, respectively). Assays contained the same components as described for the k_{cat}/K_M determination with the addition of inhibitor (Supporting Information), and reactions were initiated by addition of 10 μL of *Tm*GH1 to a final concentration of between 2.5 and 9.1 nM. Rates were monitored for a 600 s period, unless slow onset inhibition was observed, in which case reactions were allowed to run for longer and rates were taken as the slope of the line following the slow onset. The fractional decrease of v_i/v_0 for each inhibitor was calculated (using the equation $v_i/v_0 = 1 + [I]/K_i$), and the mean K_i value was taken. The dependence of $1/K_i$ on pH was fitted to a bell-shaped ionization curve.

Results

Structural, kinetic, and thermodynamic data were collected for *Tm*GH1 with the inhibitors **1**−**18**. In each case X-ray crystallography, with data ranging from 1.65 to 2.3 Å resolution, was used to observe interactions between the inhibitors and active site residues. ITC was used to dissect the thermodynamic signature of binding, and kinetic methods were used to analyze the dependence of the inhibition constant on pH; a representative example of these data is given for glucohydroximo-1,5-lactam **9** (Figure 4). The small quantities of inhibitor available, where samples were typically about 1 mg, restricted the majority of analyses to a single temperature, and 25 °C was chosen as providing good enzyme activity (k_{cat} 18 s^{-1}, K_M (DNP-Glc) 0.17 mM, Figure 5A) and more facile calorimetry; the latter was

(42) Leatherbarrow, R. J. *GraFit Version 5*; Erithacus Software Ltd.: Horley, UK, 2001.

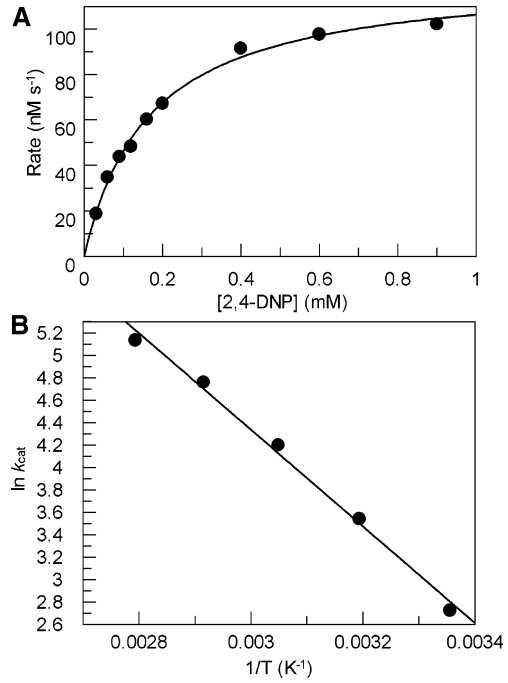

Figure 5. (A) Michaelis−Menten kinetics, rate vs substrate concentration, for the hydrolysis of 2,4-dinitrophenyl β-D-glucopyranoside by *Tm*GH1. (B) Arrhenius plot of ln k_{cat} vs $1/T$ for the same enzyme.

performed at pH 5.8, which is close to the pH optimum for catalysis (6.1 ± 0.3; this work and ref 20). The Arrhenius plot of ln k_{cat} vs $1/T$ (Figure 5B) reveals that the reaction performed by *Tm*GH1 has an enthalpy of activation of approximately 8.6 kcal mol^{-1}, consistent with values obtained on related systems,[18] compared to 29.7 kcal mol^{-1} which was determined for the uncatalyzed hydrolysis of methyl β-D-glucopyranosides.[1] As Wolfenden has shown, these relative values demand that the comparative rate enhancement through enzymatic catalysis increases sharply as the temperature decreases,[18] with implications for transition-state mimicry discussed below.

A Library of 18 Glycosidase Inhibitors. Compounds **1**−**18** fall loosely into two categories: those that are likely to be protonated and hence may mimic the charge which forms at the transition state (but which are found in a relaxed chair conformation in solution, **1**−**7**), and those which contain sp^2 hybridization and are "distorted" away from the $^4C_1$ chair conformation in a manner that may mimic the geometry of the transition state (**8**−**18**). Deoxynojirimycin **1** has served as the paradigm of glycosidase inhibition since it was first synthesized in the 1960s,[43] and while it is widely assumed to be bound to the enzyme as its conjugate acid, pH profiles and even atomic resolution crystallographic analyses leave this question unanswered.[44] Bols and colleagues subsequently pioneered the synthesis of compounds with a nitrogen atom in place of the anomeric carbon,[45−53] such as isofagomine **2**, noeuromycin **3**, tetrahydrooxazine **4**, and azafagomine **5**.

The atomic resolution structure of **2** in complex with an endoglucanase revealed unequivocally that **2** binds as its conjugate acid, with clear electron density observed for both hydrogen atoms on the nitrogen in the crystallographic analysis. Interestingly, in this form, **2** most likely interacts with an enzyme active center in which both the acid/base and nucleophile are found in their carboxylate forms.[54] Compound **4** is unlikely to be protonated, with a pK_a of 3.6,[50] but does incorporate an endocyclic oxygen in the position found in native glycosides, which is missing in all other inhibitors, and is likely to be important for binding and catalysis in the natural substrate. Compounds **2** and **4** both lack a hydroxyl group at C2, but it is clear that such an interaction is extremely important for stabilization of the transition state.[55] Castanospermine **6** and calystegine B_2 **7** both incorporate a two-carbon bridge, which causes conformational restrictions. Furthermore, **7** could, in theory, bind in one of two possible orientations.

Isofagomine lactam **8** was originally synthesized on the premise of incorporating, in a tautomeric form, a hydroxyl group at C2 and a double bond between the nitrogen and C2,[56] but atomic resolution crystallographic studies on the xylobio-derived form clearly demonstrated that the energetically favored amide form, in a $^4H_5$ conformation, is adopted.[57] *Gluco*-derived **9** and *galacto*-derived hydroximo-1,5-lactam **10** possess conjugation between the endocyclic and exocyclic nitrogen atoms, causing the 'glycoside' to take a $^4H_3$ (half chair) conformation.[29] Vasella and co-workers pioneered the fusion of tetrazole or imidazole rings to a 'glycoside' to introduce sp^2 hybridization along the bond between the anomeric carbon and nitrogen atom in place of the endocyclic oxygen atom, to generate compounds such as glucotetrazole **11** and glucoimidazole **12**.[32,33] Functional groups have been incorporated into the glucoimidazole scaffold, such as phenylethyl **13**, phenylaminomethyl **14**, methoxycarbonyl **15**, methoxycarbonylmethyl **16**, carboxylate **17**, and carboxymethyl **18** groups. Such groups were incorporated to interact with residues in the +1 subsite of the active site and thus increase potency; indeed, these compounds have been among the most potent inhibitors of β-glucosidases reported.[34] A key feature of the hydroximolactam- and glucoimidazole-derived compounds, in addition to their $^4H_3/^4E$ conformations, is that they possess a heteroatom in the ring plane, which should promote strong hydrogen bond interactions with the acid/base residue, and mimic the "lateral protonation" that occurs during catalysis.[12,58]

The pH Dependence of Inhibition Constant. The pH dependence of inhibition was measured for compounds **1**−**18** (Figure 6). As an internal control, the calorimetric K_d was also determined close to the pH optimum for catalysis (described

(43) Paulsen, H.; Sangster, I.; Heyns, K. *Chem. Ber.* **1967**, *100*, 802−815.
(44) Gloster, T.; Williams, S. J.; Roberts, S.; Tarling, C. A.; Wicki, J.; Withers, S. G.; Davies, G. J. *Chem. Commun.* **2004**, 1794−1795.
(45) Andersch, J.; Bols, M. *Chem. Eur. J.* **2001**, *7*, 3744−3747.
(46) Bols, M. *Acc. Chem. Res.* **1998**, *31*, 1−8.
(47) Jespersen, T. M.; Bols, M. *Tetrahedron* **1994**, *50*, 13449−13460.
(48) Jespersen, T. M.; Dong, W.; Sierks, M. R.; Skrydstrup, T.; Lundt, I.; Bols, M. *Angew. Chem., Int. Ed.* **1994**, *33*, 1778−1779.
(49) Liu, H. Z.; Liang, X. F.; Søhoel, H.; Bülow, A.; Bols, M. *J. Am. Chem. Soc.* **2001**, *123*, 5116−5117.
(50) Bach, P.; Bols, M. *Tetrahedron Lett.* **1999**, *40*, 3461−3464.
(51) Bols, M.; Hazell, R. G.; Thomsen, I. B. *Chem. Eur. J.* **1997**, *3*, 940−947.
(52) Ernholt, B. V.; Thomsen, I. B.; Lohse, A.; Plesner, I. W.; Jensen, K. B.; Hazell, R. G.; Liang, X.; Jakobsen, A.; Bols, M. *Chem. Eur. J.* **2000**, *6*, 278−287.
(53) Liang, X.; Bols, M. *J. Org. Chem.* **1999**, *64*, 8485−8488.
(54) Varrot, A.; Tarling, C. A.; Macdonald, J. M.; Stick, R. V.; Zechel, D. L.; Withers, S. G.; Davies, G. J. *J. Am. Chem. Soc.* **2003**, *125*, 7496−7497.
(55) Namchuk, M. N.; Withers, S. G. *Biochemistry* **1995**, *34*, 16194−16202.
(56) Williams, S. J.; Notenboom, V.; Wicki, J.; Rose, D. R.; Withers, S. G. *J. Am. Chem. Soc.* **2000**, *122*, 4229−4230.
(57) Gloster, T.; Williams, S. J.; Tarling, C. A.; Roberts, S.; Dupont, C.; Jodoin, P.; Shareck, F.; Withers, S. G.; Davies, G. J. *Chem. Commun.* **2003**, *8*, 944−945.
(58) Vasella, A.; Davies, G. J.; Böhm, M. *Curr. Opin. Chem. Biol.* **2002**, *6*, 619−629.

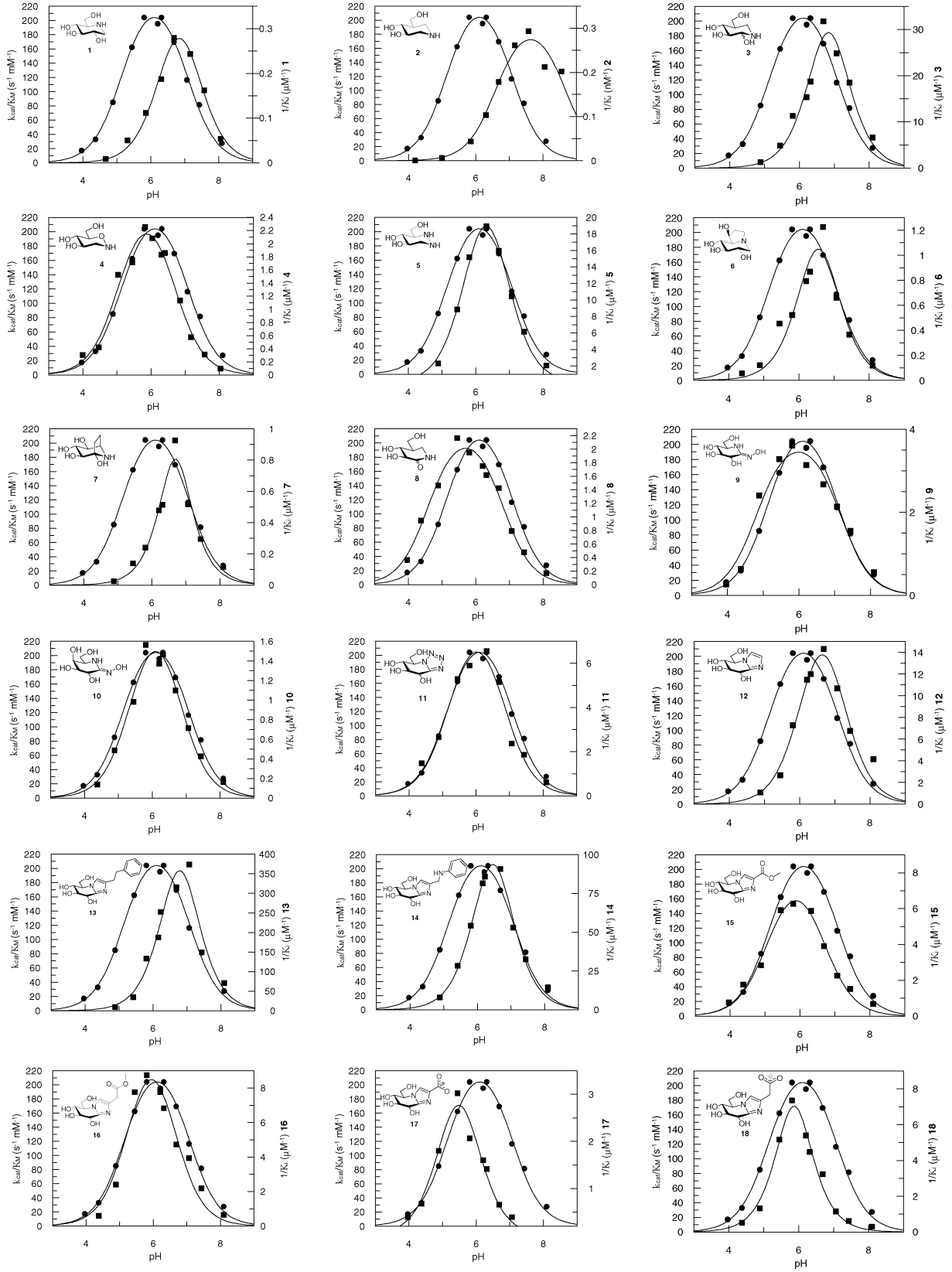

Figure 6. pH profiles of inhibition for compounds **1**−**18** with *Tm*GH1 (filled squares). Each graph also shows the pH profile of k_{cat}/K_M for *Tm*GH1 (filled circles) as a reference.

below) and in all cases agrees very well with the kinetic determination of K_i (Table 1). Slow onset inhibition, where there is an initial high catalytic rate in the presence of an inhibitor followed by a lower steady-state rate after an amount of time, was observed with almost all of the inhibitors studied here; the noticeable exceptions were **1**, **4**, and **7**. It has been suggested that the initial high rate may represent formation of the enzyme−inhibitor complex, which then undergoes conformational and

Table 1. Binding and Thermodynamic Data for Glycosidase Inhibitors **1**−**18** Bound to *Tm*GH1[a]

	K_i pH 5.8	K_i inhibition optimum	K_d	$\Delta H°_a$	$T\Delta S°_a$	pK_a1	pK_a2	pK_a of inhibitor	PDB code
13[f]	7.5 nM	2.8 nM (pH 6.8)	9.6 nM	−4.64	+6.29	6.7	6.9	6.03[34]	2CET
14	18.4 nM	10.7 nM (pH 6.4)	10.8 nM	−8.44	+2.42	6.2	6.7	5.62[35]	2J7C
16	114 nM	114 nM (pH 6.1)	48 nM	−8.82	+1.16	5.3	6.5	5.03[36]	2J7E
2[b]	23 nM	4 nM (pH 7.8)	51 nM	−6.27	+3.68	6.6	8.7	8.4[85]	1OIF
12[f]	138 nM	74 nM (pH 6.6)	56 nM	−8.96	+0.94	6.2	7.1	6.12[86]	2CES
5	66 nM	53 nM (pH 6.4)	65 nM	−11.00	−2.02	5.8	6.8	ND	2J7H
15	160 nM	160 nM (pH 5.9)	74 nM	−7.49	+2.27	6.1	6.7	ND	2J7D
18	136 nM	136 nM (pH 5.5)	100 nM	−10.71	−1.16	5.1	5.8	6.4[36]	2J7G
3	88 nM	37 nM (pH 6.8)	225 nM	−9.09	−0.90	6.6	7.0	ND	2J75
11	174 nM	174 nM (pH 5.8)	240 nM	−11.32	−2.29	5.2	6.8	−4.0[86]	2J7B
8[e]	513 nM	500 nM (pH 5.7)	290 nM	−13.55	−4.63	4.6	6.8	ND	1UZ1
9	277 nM	277 nM (pH 5.9)	384 nM	−7.02	+1.73	4.8	7.2	4.8[87]	2J78
17	485 nM	361 nM (pH 5.9)	445 nM	−8.98	−0.32	5.7	6.1	4.95[36]	2J7F
4[c]	444 nM	444 nM (pH 5.8)	541 nM	−10.51	−1.96	5.1	6.7	3.6[50]	1W3J
10	640 nM	640 nM (pH 6.0)	1.1 μM	−5.74	+2.40	5.4	6.8	5.8[30]	2J79
6[d]	2 μM	0.95 μM (pH 6.6)	2.1 μM	−6.09	+1.65	6.3	6.8	6.0[67]	2CBU
7[d]	4 μM	1.25 μM (pH 6.8)	3.3 μM	−2.94	+4.54	6.0	7.4	ND	2CBV
1[b]	9 μM	4 μM (pH 6.9)	12.9 μM	−4.60	+2.07	6.4	7.2	6.3[88]/6.7[85]	1OIM/2J77

[a] K_i values at approximately the pH optimum for *Tm*GH1 catalysis (pH 5.8[20]−6.1; this work) and at the optimum for inhibition (K_i inhibition optimum) obtained using kinetic methods, K_d values obtained using ITC, $\Delta H°_a$ and $T\Delta S°_a$ values (in kcal mol^{-1}) obtained using ITC, pK_a values from fitting to a bell-shaped curve for pH dependence of inhibition, pK_a of the inhibitor (ND, not determined), and PDB code from deposition of structural coordinates. The table is ranked by K_i value at the catalytic pH optimum, with the most potent inhibitor at the top. [b] Published in ref 20. [c] Published in ref 22. [d] Published in ref 23. [e] Published in ref 24. [f] Published in ref 21.

isomerization changes to form a more potent species.[59−62] We have speculated that these "isomerizations" may simply represent proton transfer to and from both inhibitor and protein, and subsequent remodeling of the water networks, as many of the inhibitors bind as their conjugate acids. Furthermore, many inhibitors are observed bound to a form of the enzyme not normally present in significant levels in solution, such as those with reversed protonation states for the catalytic apparatus[57] or those requiring both acid/base and nucleophile to be ionized.[20] Schramm has proposed that slow onset inhibition is actually a *bona fide* criterion for transition-state mimicry, postulating that since the enzyme is conformationally optimized to bind, initially, to the ground-state substrate, the active site thus requires conformational changes to allow tight binding to a true transition-state mimic.[5]

A preliminary inspection of the relative K_i values shows that glucoimidazoles **13** and **14** are the most potent of the inhibitors studied, with K_i values of 7.5 and 18.4 nM, respectively, at the pH for optimum *Tm*GH1 catalytic activity. Indeed the panel of glucoimidazole-derived compounds are all among the most potent of the inhibitors studied, with K_i values ranging from 7.5 nM to 485 nM. With the notable exception of isofagomine **2**, with a K_i value of 23 nM, the majority of the compounds studied here, which favor a relaxed chair conformation in solution, tend to be less potent than those which attempt to mimic the transition-state geometry.

*Tm*GH1 has a pH optimum of approximately 6.1 ± 0.3 (our previous analysis gave 5.8 ± 0.2[20] with acid and basic limbs for catalysis with pK_a values of approximately 5.3 and 7.0, respectively). The most likely interpretation of the bell-shaped pH profile for catalysis is that it simply represents titration of the catalytic acid/base and nucleophile, respectively. Of the compounds studied, a spectrum of pH profiles for inhibition is observed ranging from those which correlate perfectly with k_{cat}/K_M (such as tetrahydrooxazine **4** and both *gluco*- and *galacto*-hydroximo-1,5-lactams **9** and **10**) as well as a number of other shifts in profile. Deoxynojirimycin **1**, isofagomine **2**, noeuromycin **3**, azafagomine **4**, calystegine B_2 **7**, glucoimidazole **12**, and the phenylethyl- and phenylaminomethyl-substituted glucoimidazoles **13** and **14** all show alkaline shifts of the acid leg relative to k_{cat}/K_M. Of these, all except isofagomine **2** show a similar alkaline leg pH profile, in which the fall of K_i reflects that of k_{cat}/K_M. Compound **2** additionally shows a strong alkaline shift in its alkaline leg, which in light of atomic resolution crystallographic analyses has previously been interpreted as reflecting the conjugate acid of **2** binding to an enzyme in which both acid/base and nucleophile are in their carboxylate forms.[54] As Knowles,[63] among others, has stated, interpretation of the pH dependence on $1/K_i$ is notoriously difficult, reflecting as it does a composite of the enzyme, inhibitor, and enzyme−inhibitor complex behaviors. However, in light of the atomic resolution X-ray crystallographic analyses of both cellobio-derived imidazole[64] and cellobio-derived isofagomine,[54] it seems likely that the alkaline shift of the acid leg simply reflects the fact that a protonated inhibitor cannot bind tightly to an enzyme in which the acid/base is also protonated, for both steric and charge reasons. The second dominant difference in pH profile is displayed primarily by the carboxy-substituted imidazoles **17** and **18**, and to a lesser extent by their methoxycarbonyl analogues **15** and **16**. These compounds all show an unusual acid shift of their alkaline legs to pK_a values of ∼6, the reasons for which are harder to establish with any certainty; this may reflect either a change in acid/base pK_a or the titration of the inhibitor imidazolinium ions, whose free pK_a values are 5.0, 5.0, and 6.4 for compounds **16**−**18**, respectively (the pK_a for **15** has not been determined).

Three-Dimensional Structures of *Tm*GH1 in Complex with the Inhibitor Library. The three-dimensional structures of compounds **1**−**18** were determined in complex with *Tm*GH1; the observed electron density for the complexes that have not

(59) Morrison, J. F. *Trends Biochem. Sci.* **1982**, *7*, 102−105.
(60) Morrison, J. F.; Walsh, C. T. *Adv. Enzymol. Relat. Areas Mol. Biol.* **1988**, *61*, 201−301.
(61) Schloss, J. V. *Acc. Chem. Res.* **1988**, *21*, 348−353.
(62) Sculley, M. J.; Morrison, J. F.; Cleland, W. W. *Biochim. Biophys. Acta* **1996**, *1298*, 78−86.
(63) Knowles, J. R. *Crit. Rev. Biochem.* **1976**, *4*, 165−173.
(64) Varrot, A.; Schulein, M.; Pipelier, M.; Vasella, A.; Davies, G. J. *J. Am. Chem. Soc.* **1999**, *121*, 2621−2622.

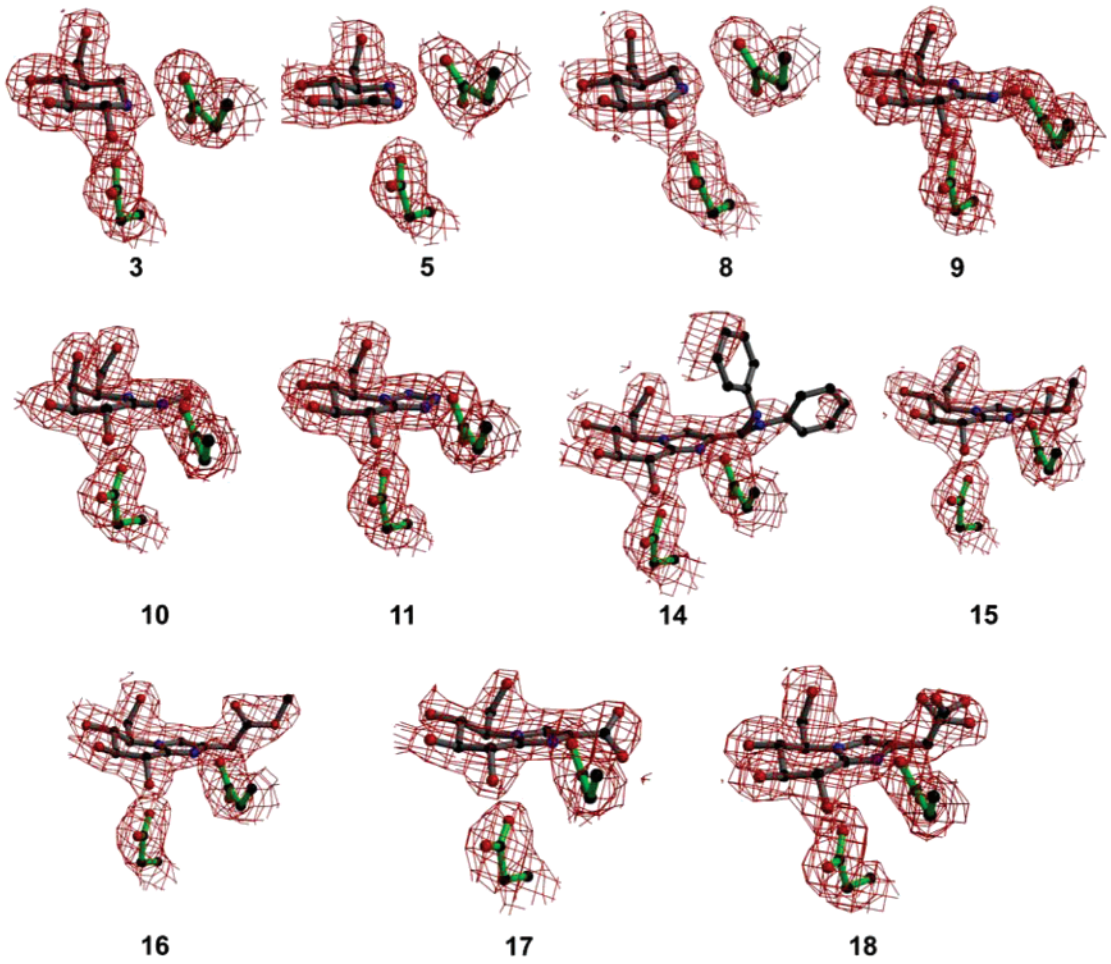

Figure 7. Observed electron density for compounds **3**, **5**, **8**−**11**, and **14**−**18** bound to the *Tm*GH1 β-glucosidase [the nucleophile Glu351 (bottom) and acid/base Glu166 (right) are shown in each case]. Electron density maps shown are maximum likelihood weighted $2F_{obs} - F_{calc}$ syntheses contoured at 1σ ($\sim$0.25 e Å^{-3}); figures were drawn using BOBSCRIPT.[83] Structures of *Tm*GH1 in complex with the other inhibitors have been reported previously.[20−24]

been described previously is shown in Figure 7. The majority of the interactions made with active site residues are invariant and thus essentially as shown in Figure 4 for the complex of *Tm*GH1 with **9**. Compounds **2**, **3**, **4**, **5**, and **7** bind in a relaxed $^4C_1$ chair conformation, whereas deoxynojirimycin **1** is distorted toward a $^1S_3$ (skew boat) conformation (in three out of four independent observations; in the other it appears as a $^4C_1$ conformation). Noeuromycin **3**, which is capable of numerous rearrangements in solution, is seen bound in its *gluco*-form. Castanospermine **6** is bound in a $^{1,4}B$ boat conformation; this ring distortion, away from that seen in the small molecule crystal structures,[65−67] and which is also observed with **1**, reflects the distortion seen in Michaelis complexes prior to the transition state, as seen with substrates in complex with other enzymes.[68,69] Compound **8** binds in a $^4H_5$ conformation, **9** and **10** bind in a $^4H_3$ conformation, and glucotetrazole **11** and all glucoimidazoles, **12**−**18**, bind in a ^4E envelope conformation. The hydroxyl group at C6 of all inhibitors interacts with Glu405 and in some cases with a water molecule. The hydroxyl group at C4 also interacts with Glu405, with the amine group of Gln20, and in some inhibitors is also close enough to interact with Trp398. Gln20, Trp406, and His121 form hydrogen bond interactions with the C3-linked hydroxyl group. Inhibitors which possess a hydroxyl group or a carbonyl group at C2 (i.e., all except **2**, **4**, and **5**) interact with Asn165 and the nucleophile, Glu351 (either one or both oxygen atoms), while some also hydrogen bond with His121. Inhibitors that possess a heteroatom at the position of the endocyclic oxygen atom are observed either to hydrogen bond with a water molecule (**1**, **4**, and **5**), or else ring distortion is observed, which allows interaction with the nucleophile (**6**, **9**, and **10**) and/or with Tyr295 (**9** and **10**). Compounds with a heteroatom at the position of the anomeric carbon (**2**, **3**, **4**, **5**, **7**, and **8**) are within hydrogen-bonding distance of both the nucleophile and acid/base residue (one oxygen atom only). The hydroximolactam, glucotetrazole, and glucoimidazole inhibitors, which have a nitrogen atom adjacent to the anomeric carbon, interact with both oxygen atoms of the acid/base residue, Glu166. The hydoximolactam and tetrazole groups interact with water molecules, as does the nitrogen atom of the glucoimidazole **12** and the carboxylate groups of **17** and **18.** It is important to note here that none of the modified glucoimidazole inhibitors (**13**−**18**) make any noncovalent interactions with active site

(65) Hempel, A.; Camerman, N.; Mastropaolo, D.; Camerman, A. *J. Med. Chem.* **1993**, *36*, 4082−4086.
(66) Hohenschutz, L. D.; Bell, E. A.; Jewess, P. J.; Leworthy, D. P.; Pryce, R. J.; Arnold, E.; Clardy, J. *Phytochemistry* **1981**, *20*, 811−814.
(67) Reymond, J.-L.; Pinkerton, A. A.; Vogel, P. *J. Org. Chem.* **1991**, *56*, 2128−2135.
(68) Davies, G. J.; Mackenzie, L.; Varrot, A.; Dauter, M.; Brzozowski, A. M.; Schülein, M.; Withers, S. G. *Biochemistry* **1998**, *37*, 11707−11713.
(69) Sulzenbacher, G.; Driguez, H.; Henrissat, B.; Schülein, M.; Davies, G. J. *Biochemistry* **1996**, *35*, 15280−15287.

residues *via* their appended functional groups. This is perhaps one of the most surprising features of the glucoimidazole series of inhibitors, which were originally synthesized on the premise of interacting with residues in the +1 subsite. Indeed, favorable hydrophobic interactions of a tryptophan residue in the +1 subsite of the active site of a family 3 glucohydrolase were observed when in complex with either **14** or a phenyl-substituted glucoimidazole compound.[70,71]

Calorimetric Dissection of Binding Thermodynamics. In an attempt to glean some thermodynamic insight into inhibitor binding, isothermal titration calorimetry was used to measure, experimentally, the $\Delta H°_a$ of ligand binding to *Tm*GH1 for all inhibitors studied (Table 1). Sample availability meant that only a single temperature and single pH (and buffer) could be accessed for the vast majority of compounds, and, for internal consistency with kinetics, a temperature of 25 °C and pH of 5.8 were chosen. Citrate buffer was chosen in order to minimize heat of ionization effects (it has a heat of ionization of −0.81 kcal mol^{-1}, which is comparable to phosphate buffer with a ΔH_{ion} of 0.86 kcal mol^{-1}).[72] For the most extreme case, ITC performed in buffers with different heats of ionization with isofagomine **2** has already shown that a single proton is released with an observed effect of approximately +0.7 kcal mol^{-1} on the $\Delta H°_a$ value obtained with citrate buffer.[20] For compounds **1**, **2**, **4**, **6**, **8**, and **12**, we were able to perform ITC at a range of different temperatures. The van't Hoff plot of ln K_a vs $1/T$ (Figure 8A) yields $\Delta H°_a$ values in good agreement (within 20% in all cases) with those determined directly by calorimetry at a single temperature.

Wolfenden has eloquently advanced the idea that true transition-state mimics would bind with a large negative enthalpy, as is true of the real transition state.[17,18] All of the inhibitors studied here indeed bind with a favorable enthalpy term. Simplistic examination of the enthalpy values alone would suggest that **4**, **8**, **11**, and **18** are good inhibitors and perhaps the most likely candidates for transition-state mimics. In contrast, however, the binding of **2** and **13** appears to be primarily governed by entropy, and yet these are two of the most potent compounds studied. The fact that entropy is, apparently, a large contributing factor to binding with many of these compounds leads to questions about whether they are true mimics of the transition state. Unfavorable entropic terms are characteristic of solvent coordination and/or conformational flexibility, and this is reflected in more favorable entropy values for **2** and **13**, when compared to **1**, **4**, and **5**, which coordinate water molecules, and for **7**, which unlike **6** does not appear to become distorted upon binding to the enzyme.

Enthalpy−entropy compensation plots are a standard way of examining related compounds, although such plots do encounter controversy in the literature.[73−76] Plotting the calorimetric data for the 18 compounds examined in this study produces an enthalpy−entropy compensation correlation (Figure 8B) with a slope of 0.93 and R^2 of 0.91. Those inhibitors that are "worse than the average" lie above the line of best fit, whereas those that are "better than average" fall below. Consistent with the kinetically determined K_i values, those compounds which are conformationally restricted to a transition-state mimicking geometry (^4E and $^4H_3$ conformations) dominate the "better than average" inhibitors, but there are clear exceptions, notably (again) the tight binding of isofagomine **2**.

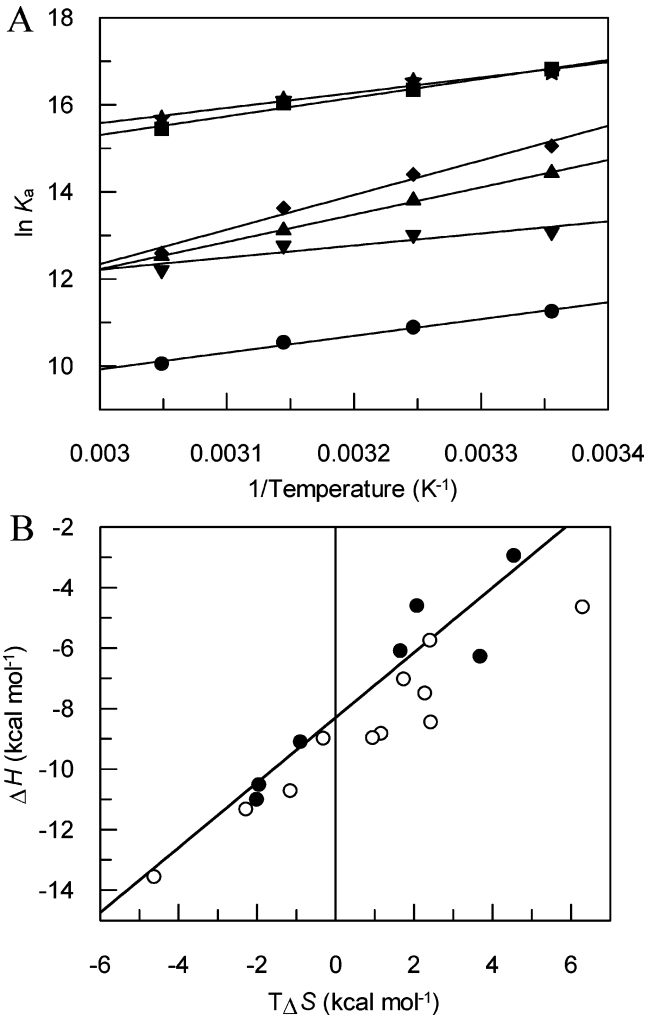

Figure 8. (A) van't Hoff plot of ln K_a vs $1/T$ for inhibitors **1** (circles), **2** (squares), **4** (triangles), **6** (inverted triangles), **8** (diamonds), and **12** (stars). (B) Enthalpy−entropy compensation plot for all inhibitors studied with *Tm*GH1 using the data shown in Table 1; compounds **1**−**7** are shown in filled circles and those containing sp^2 hybridization (**8**−**18**) with open circles. The line of best fit has a gradient of 0.93 and a correlation coefficient of 0.91.

Discussion

The potency of glycosidase inhibitors appears to have been stuck in the micromolar to nanomolar range since their discovery in the 1960 or 1970s. Recent developments in synthetic methods, computer-aided design and techniques such as those used in the course of this study have allowed inhibitor design and characterization to progress, but there still remains great controversy about what constitutes a transition-state mimic. Wolfenden has observed that the temperature dependence of enzymatic catalysis implies not only that the rate enhancement through enzymatic catalysis increases sharply as the temperature decreases, but also that true transition-state mimics should behave similarly and show a correspondingly sharp temperature

(70) Hrmova, M.; de Gori, R.; Smith, B. J.; Vasella, A.; Vargese, J. N.; Fincher, G. B. *J. Biol. Chem.* **2004**, *279*, 4970−4980.
(71) Hrmova, M.; Streltsov, V. A.; Smith, B. J.; Vasella, A.; Vargese, J. N.; Fincher, G. B. *Biochemistry* **2005**, *44*, 16529−16539.
(72) Goldberg, R.; Kishore, N.; Lennen, R. *J. Phys. Chem. Ref. Data* **2002**, *31*, 231−370.
(73) Dunitz, J. D. *Chem. Biol.* **1995**, *2*, 709−712.
(74) Sharp, K. *Protein Sci.* **2001**, *10*, 661−667.
(75) Cooper, A. *Curr. Opin. Chem. Biol.* **1999**, *3*, 557−563.
(76) Cornish-Bowden, A. *J. Biosci.* **2002**, *27*, 121−126.

dependence on K_i, which is of course reflected directly in their $\Delta H°_a$ of binding. It is clear that the $\Delta H°_a$ values observed here, either by direct calorimetry measurement for compounds **1**−**18**, or equally through van't Hoff analysis of **1**, **2**, **4**, **6**, **8**, and **12**, do not correlate with transition-state mimicry, as chemically similar compounds behave quite differently. That pH dependence on k_{cat}/K_M should mirror that of $1/K_i$ has also been advanced as a feature of only true transition-state mimics,[77] but few of the compounds investigated here follow that trend; indeed, those that do are often intuitively more representative of the ground state, such as tetrahydrooxazine **4**.

Interpretation of any experimental determination of enthalpy (Figure 8) is challenging. Clearly, and in contrast to our initial preconceptions, there is no convenient correlation of either K_i or $\Delta H°_a$ with the "chemistry" of the inhibitor; both the conformationally ^4E-locked imidazoles and $^4C_1$ isofagomine **2** are among the most potent inhibitors, yet they are essentially randomly distributed across the enthalpy−entropy landscape. Glucoimidazoles, such as **13** and **14**, which differ only by the replacement of a carbon by a nitrogen atom, are found at opposite ends of the plot. The most likely discrepancy among the observed $\Delta H°_a$ values, inhibitor chemistry and the potential transition-state analogy almost certainly results from solvation and desolvation effects, which are unaccounted for in studies such as those described here; these effects have previously been shown to play substantial roles in carbohydrate chemistry and catalysis (for example refs 78, 79). As Homans,[80] in particular, has advised, both X-ray crystallographic analyses and calorimetry of complexes provide only partial insight into the binding process. Binding, rather like protein folding, results in a small favorable energy derived from the sum of exceedingly large and conflicting terms. Ligand binding, Homans observes,[80] is essentially a desolvation event in which even a single hydroxyl group can change the solute−solute free energy of binding by ∼−30 kcal mol^{-1}, which viewed in light of the overall range of $\Delta H°_a$ values of binding observed here, from ∼−3 to −14 kcal mol^{-1}, puts these enormous factors into perspective. Similarly, modeling studies (which have not yet advanced to the level required for the complex inhibitors studied here) reveal that even a shift in hydroxyl position from equatorial to axial may have significant effects on local cooperative water networks and the energetic cost of desolvation.[81] So while calorimetry gives a single $\Delta H°_a$ value, and the complexes of **1**−**18** with *Tm*GH1 a fine insight into the complexation of waters associated with binding, desolvation effects of the compounds involved likely dominate both binding and $\Delta H°_a$. As Whitesides has also recently noted,[82] having observed similar unusual behavior with ligand binding to bovine carbonic anhydrase II, understanding of the ligand binding phenomenon is essential for future rational design of high affinity ligands, yet it frequently remains paradoxical.

Acknowledgment. We would like to thank the Engineering and Physical Sciences Research Council for a Ph.D. studentship (T.M.G.) and the Biotechnology and Biochemical Sciences Research Council and the Swiss National Science Foundation for funding. Shirley Roberts and Elizabeth Stewart are thanked for help with crystallization and Harry Gilbert for provision of a working calorimeter and continuing useful advice.

Supporting Information Available: Full ITC, kinetic, and structural refinement details and observed calorimetric titrations. This material is available free of charge via the Internet at http://pubs.acs.org.

JA066961G

(77) Legler, G. Glycosidase inhibition by basic sugar analogs and the transition state of enzymatic glycoside hydrolysis. In *Iminosugars as glycosidase inhibitors. Nojirimycin and beyond*; Stütz, A. E., Ed.; Wiley-VCH: Weinheim, 1999; pp 31−67.
(78) Galema, S. A.; Blandamer, M. J.; Engberts, J. B. F. N. *J. Am. Chem. Soc.* **1990**, *112*, 9665−9666.
(79) Galema, S. A.; Blandamer, M. J.; Engberts, J. B. F. N. *J. Org. Chem.* **1992**, *57*, 1995−2001.
(80) Daranas, A.; Shimizu, H.; Homans, S. *J. Am. Chem. Soc.* **2004**, *126*, 11870−11876.
(81) Dashnau, J. L.; Sharp, K. A.; J. M. V. *J. Phys. Chem. B* **2005**, *109*, 24152−24159.
(82) Krishnamurthy, V. M.; Bohall, B. R.; Semetey, V.; Whitesides, G. M. *J. Am. Chem. Soc.* **2006**, *128*, 5802−5812.
(83) Esnouf, R. M. *J. Mol. Graph. Model.* **1997**, *15*, 132−134.
(84) Merritt, E. A.; Murphy, M. E. P. *Acta Crystallogr. D Biol. Crystallogr.* **1994**, *50*, 869−873.
(85) Jensen, H. H.; Lyngbye, L.; Bols, M. *Angew. Chem., Int. Ed.* **2001**, *40*, 3447−3449.
(86) Panday, N.; Vasella, A. *Synthesis* **1999**, SI, 1459−1468.
(87) Hoos, R.; Vasella, A.; Rupitz, K.; Withers, S. G. *Carbohydr. Res.* **1997**, *298*, 291−298.
(88) Dale, M. P.; Ensley, H. E.; Kern, K.; Sastry, K. A. R.; Byers, L. D. *Biochemistry* **1985**, *24*, 3530−3539.